Electronic Spectra of PS I Mutants: The Peripheral Subunits Do Not Bind Red Chlorophylls in *Synechocystis* sp. PCC 6803

Victor Soukoulis,* Sergei Savikhin,* Wu Xu,# Parag R. Chitnis,# and Walter S. Struve*
*Ames Laboratory, U. S. Department of Energy, and Department of Chemistry and #Department of Biochemistry and Biophysics, Iowa State University, Ames, Iowa 50011 USA

ABSTRACT Steady-state fluorescence and absorption spectra have been obtained in the Q_y spectral region (690–780 nm and 600–750 nm, respectively) for several subunit-deficient photosystem I mutants from the cyanobacterium *Synechocystis* sp. PCC 6803. The 77 K fluorescence spectra of the wild-type and subunit-deficient mutant photosystem I particles are all very similar, peaking at ~720 nm with essentially the same excitation spectrum. Because emission from far-red chlorophylls absorbing near 708 nm dominates low-temperature fluorescence in *Synechocystis* sp., these pigments are not coordinated to any the subunits PsaF, Psa I, PsaJ, PsaK, PsaL, or psaM. The room temperature (wild-type–mutant) absorption difference spectra for trimeric mutants lacking the PsaF/J, PsaK, and PsaM subunits suggest that these mutants are deficient in core antenna chlorophylls (Chls) absorbing near 685, 670, 675, and 700 nm, respectively. The absorption difference spectrum for the PsaF/J/I/L-deficient photosystem I complexes at 5 K reveals considerably more structure than the room-temperature spectrum. The integrated absorbance difference spectra (when normalized to the total PS I Q_y spectral area) are comparable to the fractions of Chls bound by the respective (groups of) subunits, according to the 4-Å density map of PS I from *Synechococcus elongatus*. The spectrum of the monomeric PsaL-deficient mutant suggests that this subunit may bind pigments absorbing near 700 nm.

INTRODUCTION

Photosystem I (PS I) is a pigment-protein complex embedded in the photosynthetic membranes of higher plants, cyanobacteria, and algae (Brettel, 1997). It utilizes light to generate NADPH and reduced ferrodoxin; these reductants in turn drive many biochemical processes, such as the Calvin cycle, reduction of nitrite to ammonia, glutamate synthesis, and enzyme regulation (Chitnis, 1996).

This paper is concerned with the spatial distribution of chlorophyll *a* (Chl *a*) spectral forms in the core antenna of PS I. Analyses of steady-state absorption spectra suggest that the ~100 bulk antenna pigments comprise several distinct Chl spectral forms, with Q_y band maxima ranging between 650 and 700 nm (Ikegami and Itoh, 1986; Owens et al., 1988; Jia et al., 1992; Gobets et al., 1994). Kinetic experiments have pointed to the presence of an additional, smaller pool (2–10 Chls) of specialized pigments, which absorb to the red of the P700 lower exciton component (Holzwarth et al., 1990; Turconi et al., 1993; Hastings et al., 1995). The number and type of these far-red pigments (hereafter termed "red Chls" to distinguish them from the bulk antenna Chls) reportedly depend on the species. Hastings et al. (1995) estimated that the core antennas of cyanobacteria contain ~10 red Chls absorbing at 690–700 nm. Gobets et al. (1994) concluded that *Synechocystis* sp. PCC 6803 exhibits only two red Chls, which exhibit a 708-nm absorption band maximum at low temperatures. Several authors (Werst et al., 1992; Trinkunas and Holzwarth, 1994; Jia et al., 1992) have suggested that these red Chls are adjacent to the reaction center and serve to localize excitations toward the reaction center. The distribution of the remaining, bulk Chl spectral forms has not been established. Possible arrangements range between a funnel model (bluest-absorbing Chls on the periphery, with downhill energy gradients toward the reaction center) and a model in which the spectral forms are randomly distributed about the reaction center.

In this work we have obtained low-temperature fluorescence and fluorescence excitation spectra of several subunit-deficient photosystem I mutants from *Synechocystis* sp. PCC 6803. We have also analyzed the wild-type–mutant absorption difference spectra for most of the mutants at room temperature and for the PsaF/J/I/L-deficient mutant at 5 K. The fluorescence spectra prove that none of the peripheral subunits bind the red Chls, because the 720-nm low-temperature fluorescence band (characteristic of the red Chls) is intact in all of the mutants. The absorption difference spectra suggest that the spatial distribution of Chl spectral forms is essentially random.

MATERIALS AND METHODS

Different PS I preparations were isolated from the wild-type and mutant strains of the cyanobacterium *Synechocystis* sp. PCC 6803 (Table 1). *Synechocystis* sp. PCC 6803 cells were cultured in a BG11 medium with aeration under 40 $\mu mol^{-1}\ m^{-1}$ light intensity at 30°C. Cells were harvested at the late exponential phase and centrifuged at 5000 × *g*. Pellets were resuspended in SMN buffer (0.4 mM sucrose, 10 mM NaCl, 50 mM 3-(*N*-morpholino)propanesulfonic acid, pH 7.0) and were stored at −20°C until further use. Before lysis, cells were thawed at room temperature, and

Received for publication 30 November 1998 and in final form 22 February 1999.

Address reprint requests to Dr. Walter S. Struve, Department of Chemistry, Iowa State University, Gilman Hall, Ames, IA 50011-3111. Tel.: 515-294-4276; Fax: 515-294-1699; E-mail: wstruve@ameslab.gov.

0006-3495/99/05/2711/05 $2.00

TABLE 1 Strains of *Synechocystis* sp. PCC 6803 used in this study

Strain	Description	Characteristics of the isolated PSI complexes
Wild type	Glucose-tolerant strain	Eleven subunits resolved electropheretically
AFK6	*psaF* replaced by a kanamycin resistance gene; *psaJ* transcriptionally inactivated (Xu et al., 1994)	PsaF and PsaJ missing and level of PsaE decreased (Xu et al., 1994)
ALC7	*psaL* replaced by a chloramphenicol resistance cartridge (Chitnis et al., 1993)	PsaL absent; unable to form PSI trimers (Chitnis and Chitnis, 1993)
AMS13	*psaM* replaced by a spectinomycin resistance cartridge (P. R. Chitnis, unpublished results)	PsaM absent
K1K2	*psaK1* and *psaK2* replaced by the chloramphenicol and spectinomycin-resistance cartridges, respectively (P. R. Chitnis, unpublished results)	PsaK absent
FJI	*psaF* replaced by a kanamycin resistance gene; psaJ transcriptionally inactivated; *psaI* replaced by a chloramphenicol-resistance cartridge (P. R. Chitnis, unpublished results)	PsaF, PsaJ, PsaI, PsaL absent

the protease inhibitor phenylmethanesulfonyl fluoride was added to a final concentration of 0.2 mM. The cells were broken in a bead beater, unbroken cells were removed by centrifugation at 5000 × *g* for 30 min at 4°C, and the membranes were pelleted by centrifugation at 50,000 × *g* for 1 h at 4°C. The membranes were suspended in SMN buffer and homogenized. Trimeric and monomeric PS I complexes were prepared by a previously published method (Sun et al., 1998). Optical clarity of the PSI preparations was improved by centrifuging through Spin-X centrifuge filter units (0.22-μm cellulose acetate membrane; Costar). The chlorophyll concentration of PS I trimers was measured in 80% acetone. The purity of PS I preparations was examined by sodium dodecyl sulfate-polyacrylamide gel electrophoresis analysis of protein subunits.

Fluorescence spectra were obtained with 1-nm resolution at 77 K in an ISA Spex FluoroMax-2 spectrofluorimeter. PS I samples in buffer were diluted 2:1 with glycerol and housed in a quartz tube (4–5-mm internal diameter) immersed in liquid N_2. Sample optical densities were ~0.04 at 680 nm over a 5-mm path length.

All room-temperature absorption spectra were obtained on a Perkin-Elmer Lambda 3B UV-visible spectrophotometer and digitized in a master personal computer. Spectral manipulations (renormalization, subtraction, etc.) were performed with Spectra-Solve software (Ames Photonics, Ames, IA). Extreme care was taken to ensure the reproducibility of absorbance measurements, because fractional absorbance differences of interest were typically 1–5%. All PS I samples were either freshly prepared or had been frozen once; multiple freeze-thaw cycles changed the spectra by <1%. Samples were typically diluted to the same peak absorbance within 15% (OD ~1 at 680 nm), to minimize possible measurement nonlinearity. After ~2 h of spectrophotometer warmup, a background absorbance spectrum was taken with only buffer solution in the sample cell. A sequence of three to five absorption spectra were then taken for different mutants. In initial experiments, each wild-type (WT) or mutant spectrum was taken twice, but these proved to be so reproducible (<1%) that each sample spectrum was recorded only once. A final buffer spectrum was taken, and a weighted average of the two buffer spectra was subtracted from the raw sample spectrum. The weighting factors depended on the timing of sample spectrum accumulation, relative to the time interval between recordings of the buffer spectra. The buffer spectra were featureless in the visible region. Sample volumes were typically 120 μl in a 1-mm-path-length cell. In control experiments, absorption spectra were taken for WT samples isolated by column separation with congruent centrifugation, instead of the isolation protocol described above. These samples yielded spectra with <1% deviations from those of the earlier preparations. Absorption spectra of the wild-type and PsaF/J-deficient mutant PS I were obtained at 5 K in a liquid He immersion dewar with a Bruker IFS 120 HR high-resolution Fourier transform spectrometer used in spectral hole-burning studies (courtesy of G. J. Small and M. Rätsep).

RESULTS AND DISCUSSION

Fig. 1 shows the WT room-temperature absorption spectrum (corrected for the control buffer spectrum) in the Q_y spectral region for the PS I core antenna–reaction center complex from *Synechocystis* sp. PCC 6803. The 680-nm band maximum is dominated by the 0–0 Q_y feature of core antenna Chls. The red Chls and the P700 lower exciton component account primarily for the unresolved absorption tail at wavelengths greater than 690 nm. At room temperature, the mutant spectra deviate so little from this WT spectrum (<5% at most wavelengths) that they would be nearly indistinguishable from the WT spectrum in this figure.

The 77 K fluorescence spectra of WT PS I and its mutants lacking the PsaF/J/I, PsaK, PsaL, and PsaM subunits are shown in Fig. 2. The PsaK- and PsaM-deficient mutants are trimeric, whereas the PsaF/J/I- and PsaL-deficient mutants are monomeric. (The PsaL subunit is required for assembly of PS I trimers. The PsaI subunit also plays a role in trimer assembly, because in its absence the PsaL subunit cannot be

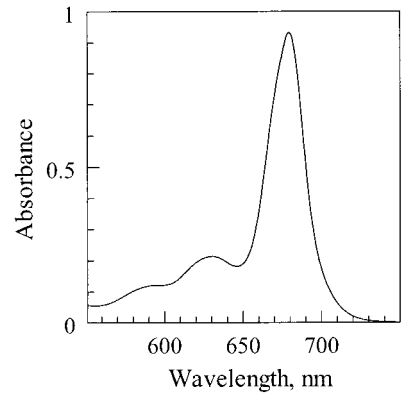

FIGURE 1 Steady-state absorption spectrum of trimeric wild-type photosystem I core antenna–reaction center complex from *Synechocystis* sp. PCC 6803. Background correction for optical cell plus buffer has been applied.

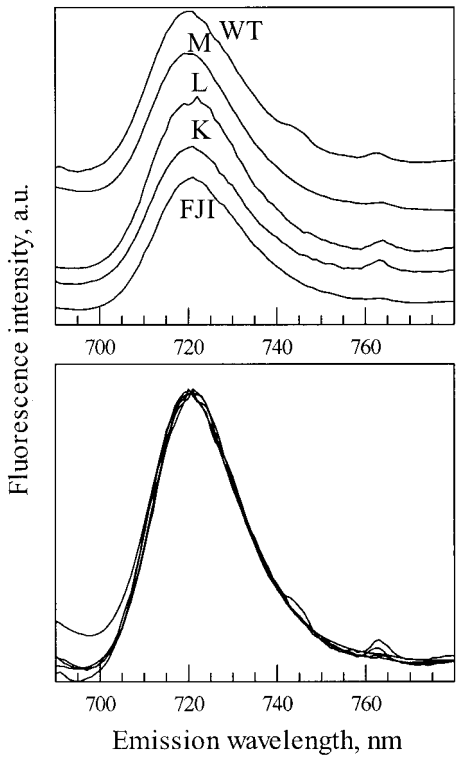

FIGURE 2 Fluorescence spectra of WT and mutant PS I core antenna–reaction center complex. Individual spectra are staggered vertically at top; superimposed spectra are shown at bottom. Excitation wavelengths are 680, 675, 650, 630, and 680 nm for WT and PsaM-, PsaL-, PsaK-, and PsaF/J/I-deficient mutants, respectively. Bumps in several spectra (e.g., near 763 nm) are spectrophotometer artifacts.

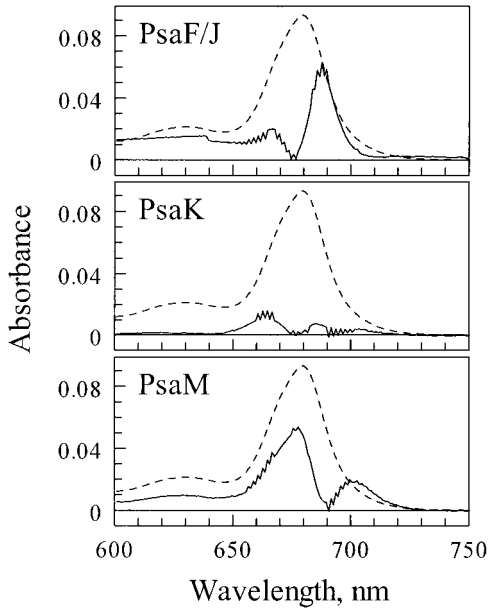

FIGURE 3 Background-corrected absorption difference spectra (WT-mutant) for PSI core antenna–reaction center complexes from mutants lacking the indicated subunits: PsaF/J, PsaK, and PsaM. Dashed curves give WT PS I absorption spectrum, scaled down by a factor of 10. Relative absorbances are given directly by the vertical scale.

incorporated into the PS I complex. Hence PS I monomers from the PsaF/J/I-deficient mutant lack the L subunit as well as the F, J, and I subunits.) All of these spectra (which peak near 720 nm) are nearly superimposable; their shapes are essentially independent of excitation wavelength between 590 and 700 nm. These spectra closely resemble the 77 K WT spectrum reported by Gobets et al. (1994), except that our spectra lack the 676-nm peak attributed by these workers to free Chls. The corresponding fluorescence excitation spectra are also very similar among the WT and mutants (not shown). Whereas they are dominated by a broad maximum at 670–680 nm, the excitation spectra also exhibit a secondary bump at 708–710 nm. The latter feature is consistent with (but does not prove) the conclusion of Gobets et al. that the 720-nm fluorescence band is emitted by pigments absorbing near 708 nm.

The room-temperature WT-mutant difference spectra for the trimeric PsaF/J-, PsaK-, and PsaM-deficient mutants are given in Fig. 3. These are superimposed on the WT spectrum, which has been scaled down by a factor of 10 for comparison. The mutual normalization for subtraction of the WT and mutant spectra is arbitrary a priori, because no technique exists for assaying relative P700 concentrations to $<1\%$ precision. Hence the digitized spectra were renormalized so that the WT-mutant difference spectra were non-negative for all wavelengths and zero for at least one. (This zero sometimes occurred outside the spectral range shown in Fig. 3.) Such a procedure would be valid if the spectral effect of subunit deletion were purely subtractive—i.e., if the local environments of Chls bound to the remaining subunits were unchanged by the mutations. The precision in the difference spectra is inherently lowest for wavelengths near the PS I band maximum; it improves for wavelengths at the peripheries. The band maxima in the difference spectra are so sharply defined (Fig. 3) that their positions are insensitive to details of normalization. If these difference spectra are taken at face value, the PsaF/J subunits appear to bind Chls with Q_y 0–0 band maximum at 685 nm; they may also bind 665 nm Chls, but it is uncertain to what extent this secondary peak is actually a vibronic feature of the main 685-nm band. The PsaM subunit appears to contain Chls absorbing at 675 nm (major) and 700 nm (minor). The difference spectrum for the PsaK-deficient mutant appears to be bimodal, with nearly equal contributions from spectral forms at ~665 and 680 nm.

Fig. 4 shows a difference spectrum between trimeric WT and monomeric PsaL-deficient PS I. This mutant does not form trimers; the PsaL subunit (which grazes the threefold rotational axis in trimeric WT and interacts closely with the PsaL subunits in neighboring monomers) appears to be essential to trimer formation. This difference spectrum suggests that PsaL contains predominantly 700-nm Chls. However, this conclusion must be regarded with more caution, because monomer-monomer interactions (absent in the PsaL-deficient mutant) may contribute to the difference spectrum.

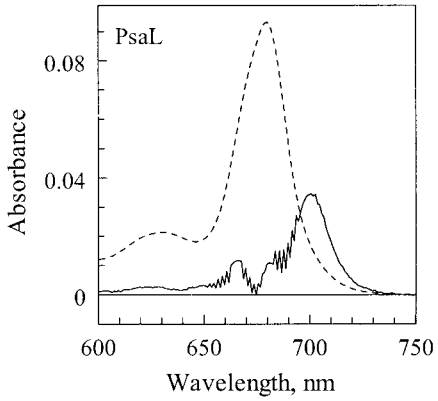

FIGURE 4 Background-corrected absorption difference spectrum (WT-mutant) for the PsaL-deficient mutant. The dashed curve is the WT PS I absorption spectrum, scaled down by a factor of 10. The vertical scale reflects relative absorbances.

When compared with the WT spectrum (~100 Chls/monomer), the integrated areas of the difference spectra suggest that the PsaF/J, PsaM, PsaK, and PsaL subunits bind ~5, 5, 1, and 2–3 Chls, respectively. Whereas these numbers are much more sensitive to our normalization procedure than the band positions, the PsaF/J, PsaK, and PsaL numbers are similar to the numbers of Chls identified as bound to the respective subunits in the density map (Krauss et al., 1996). The spectroscopic PsaM number (~5) is larger than the number of Chls bound to this subunit in the density map (1–2). Krauss et al. have identified 89 of the ~100 Chls in monomeric PS I, and their assignment of the PsaM subunit is tentative. Hence the pigment numbers in their current density map may only be a lower bound to the true Chl numbers.

The WT and PsaF/J/I-deficient absorption and difference spectra at 5 K are shown in Fig. 5. This mutant lacks the antenna Chls that are bound to subunits PsaF, J, I, and L in WT PS I. A similar subtraction protocol was used here. At this temperature, the long-wavelength features in the individual spectra are so well resolved that the WT-mutant spectral differences become discernible to the unaided eye. The room-temperature WT-mutant difference spectrum is superimposed in Fig. 5 for comparison with the 5 K difference spectrum. The 668- and 688-nm peaks in the room-temperature difference spectrum become split into peaks at 667, 672, 680, 687, 691, and 699 nm. The peak positions are so sharply defined at 5 K that they are little influenced by mutual normalization of the WT and mutant spectra.

To our knowledge, our fluorescence spectra provide the first hard evidence regarding the location of the red Chls in the three-dimensional map of the cyanobacterial PS I core antenna–reaction center complex (Krauss et al., 1996). Subunits PsaF/J, PsaK, PsaL, and PsaM are located around the periphery of the PsaA-PsaB heterodimer, which binds most of the core antenna pigments as well as the reaction center chlorophylls (Fig. 6). PsaF/J is situated on the outer perimeter of the PS I monomer and does not interact with other monomers within the trimer. PsaK and PsaM occupy boundaries between subunits, and PsaL is adjacent to the trimer C_3 axis. The F708 Chls are clearly not bound to any of these peripheral subunits, because all of the subunit-deficient mutants display physiological fluorescence spectra at low temperature. Because no other subunits appear to bind Chls besides PsaA/B (Krauss et al., 1996), the red Chls are likely to be coordinated to this heterodimer. In global analyses of ultrafast pump-probe experiments on WT *Synechosystis* sp. PS I excited at 660 nm (S. Savikhin, X. Wu, V. Soukoulis, P. R. Chitnis, and W. S. Struve, unpublished work), the equilibration between bulk and red antenna Chls is signaled by the presence of decay-associated spectral (DAS) components with lifetimes of 2.0 and 6.4 ps. The

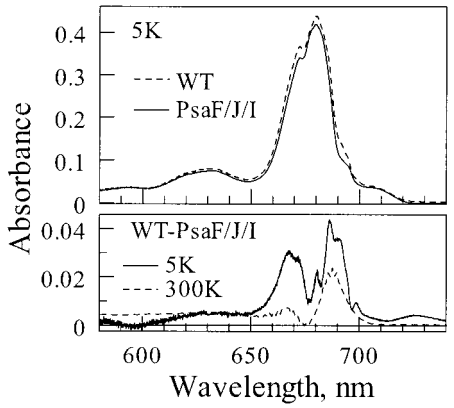

FIGURE 5 Absorption spectra at 5 K of WT and PsaF/J/I-deficient PS I from *Synechocystis* sp. PCC 6803 (*top*). The bottom panel shows (WT-mutant) absorption difference spectra at 5 K and at room temperature.

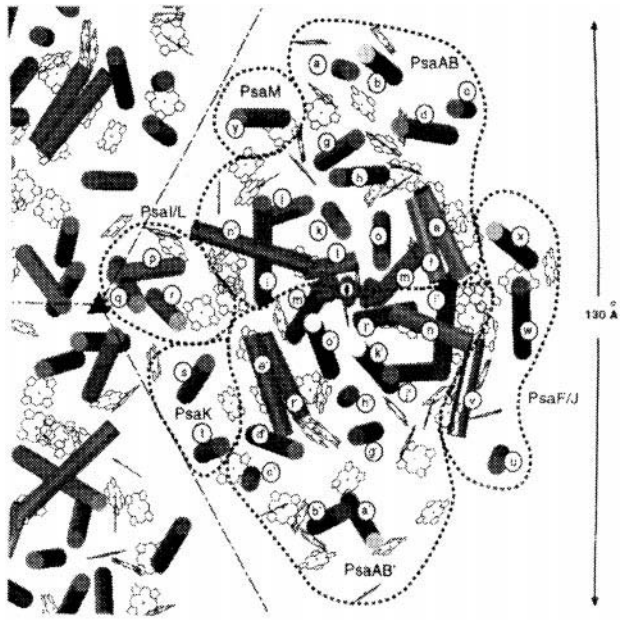

FIGURE 6 Relative locations of protein subunits in a PS I monomer (from Krauss et al., 1996; used with permission). The reaction center is located at the boundary between the PsaA and PsaB subunits.

corresponding DAS and lifetimes for the PsaF/J-deficient PS I mutant are virtually the same as for the WT, indicating that the red antenna Chl kinetics are essentially unperturbed in this mutant.

The conclusions from the absorption difference spectra in Figs. 3–5 are more speculative. The mutant strains used in this study contain active PS I complexes with the wild-type levels of the remaining subunits and normal electron transfer rates (Chitnis et al., 1993; Xu et al., 1994; Chitnis, unpublished results). As in the wild type, the PS I complexes are stable in the mutant cells. Therefore, gross changes in the PS I structure are not likely in these mutants. Yet we cannot rule out the possibility that deletion of a subunit may significantly alter the electronic spectra of Chls bound to the surviving subunits. Nevertheless, the results presented here suggest that whereas some of the bluer Chls absorbing at ~665 nm are found in peripheral subunits of the PS I monomer, so too are some of the Chls absorbing farther to the red (in the Psa L and PsaM subunits). Our results support the notion that the spatial distribution of Chl spectral forms in the core antenna is essentially random rather than vectorial. However, Chls absorbing at wavelengths greater than 700 nm do not emerge in any of our difference spectra; such Chls appear to be bound to the PsaA/B heterodimer, rather than to peripheral subunits. Kinetic modeling of recent pump-probe experiments on WT PS I from *Synechocystis* (S. Savikhin, X. Wu, V. Soukoulis, P. Chitnis, and W. S. Struve, unpublished work) predicts that positioning red of Chls on the antenna periphery has little effect on the overall efficiency of core antenna excitation trapping at the reaction center.

Note added in proof: Karapetyan et al. (Karapetyan, Dorra, Schweitzer, Bezsmertnaya, and Holzwarth (1997) *Biochemistry* 36:13830-13837) reported that a very long-wavelength fluorescence band (F760) in trimeric PSI I from *Spirulina platensis* appears with greatly reduced intensity in monomeric PS I, but is restored in reassembled trimers. Hence, this fluorescence band likely arises from interactions between peripheral Chls in different monomers. The fluorescence band described in our paper remains intact in both monomeric and trimeric subunit-deficient mutants of *Synechocytis* sp. (Fig. 2) and it is clearly not a counterpart to the F760 band in *Spirulina.*

We are indebted to G. J. Small and M. Rätsep for the use of their high-resolution absorption spectrometer and to J. Petrich for the use of the spectrofluorimeter.

The Ames Laboratory is operated for the U.S. Department of Energy by Iowa State University under contract W-7405-Eng-82. This work was supported by the Division of Chemical Sciences, Office of Basic Energy Sciences. Generation of subunit-deficient cyanobacterial mutants was supported in part by grants from the National Science Foundation (MCB#9696170 and MCB#9723001).

REFERENCES

Brettel, K. 1997. Electron transfer and arrangement of the redox cofactors in photosystem I. *Biochim. Biophys. Acta.* 1318:322–373.

Chitnis, P. R. 1996. Photosystem I. *Plant Physiol.* 111:661–669.

Chitnis, V. P., and P. R. Chitnis. 1993. PsaL subunit is required for the formation of photosystem I trimers in the cyanobacterium *Synechocystis* sp. *PCC.* 6803. *FEBS Lett.* 336:330–334.

Chitnis, V. P., Q. Xu, L. Yu, J. H. Golbeck, H. Nakamoto, D.-L. Xie, and P. R. Chitnis. 1993. Targeted inactivation of the gene PsaL encoding a subunit of photosystem I of the cyanobacterium *Synechocystis* sp. *PCC 6803. J. Biol. Chem.* 268:11678–11684.

Gobets, B., H. van Amerongen, R. Monshouwer, J. Kruip, M. Rögner, R. van Grondelle, and J. P. Dekker. 1994. Polarized site-selected fluorescence spectroscopy of isolated photosystem I particles. *Biochim. Biophys. Acta.* 1188:75–85.

Hastings, G., S. Hoshina, A. N. Webber, and R. E. Blankenship. 1995. Universality of energy and electron transfer processes in photosystem I. *Biochemistry.* 34:15512–15522.

Holzwarth, A. R., W. Haehnel, R. Ratajczak, E. Bittersmann, and G. H. Schatz. 1990. Energy transfer kinetics in photosystem I particles isolated from *Synechococcus* sp. and from higher plants. *In* Current Research in Photosynthesis. M. Baltscheffsky, editor. Kluwer Academic Publishers, Dordrecht. 611–614.

Ikegami, I., and S. Itoh. 1986. Chlorophyll organization in P-700-enriched particles isolated from spinach chloroplasts: CD and absorption spectroscopy. *Biochim. Biophys. Acta.* 851:75–85.

Jia, Y., J. M. Jean, M. M. Werst, C.-K. Chan, and G. R. Fleming. 1992. Simulations of the temperature dependence of energy transfer in the PS I core antenna. *Biophys. J.* 63:259–273.

Krauss, N., W.-D. Schubert, O. Klukas, P. Fromme, H. T. Witt, and W. Saenger. 1996. Photosystem I at 4 Å resolution: a joint photosynthetic reaction center and core antenna system. *Nature Struct. Biol.* 3:965–973.

Owens, T. G., S. P. Webb, L. Mets, R. S. Alberte, and G. R. Fleming. 1988. Antenna structure and excitation dynamics in photosystem I. I. Studies of detergent-isolated photosystem I preparations using time-resolved fluorescence analysis. *Biophys. J.* 53:733–745.

Sun, J., K. An, P. Jin, V. P. Chitnis, and P. R. Chitnis. 1998. Isolation and characterization of photosystem I subunits from the cyanobacterium *Synechocystis* sp. PCC 6803. *Methods Enzymol.* 297:124–139.

Trinkunas, G., and A. R. Holzwarth. 1994. Kinetic modeling of exciton migration in photosynthetic systems. 2. Simulations of excitation dynamics in two-dimensional photosystem I core antenna/reaction center complexes. *Biophys. J.* 66:415–429.

Turconi, S., G. Schweitzer, and A. R. Holzwarth. 1993. Temperature dependence of picosecond fluorescence kinetics of a cyanobacterial photosystem I particle. *Photochem. Photobiol.* 57:113–119.

Werst, M., Y. Jia, L. Mets, and G. R. Fleming. 1992. Energy transfer and trapping in photosystem I core antenna: a temperature study. *Biophys. J.* 61:868–878.

Xu, Q., V. P. Chitnis, L. Yu, and P. R. Chitnis. 1994. Function and organization of photosystem I in a cyanobacterial mutant strain that lacks PsaF and PsaJ subunits. *J. Biol. Chem.* 269:3205–3211.